THE JOURNAL OF BIOLOGICAL CHEMISTRY VOL. 285, NO. 21, pp. 16286–16293, May 21, 2010

Phosphorylation-induced Conformational Changes in the Retinoblastoma Protein Inhibit E2F Transactivation Domain Binding*[S]

Received for publication, January 26, 2010, and in revised form, March 10, 2010 Published, JBC Papers in Press, March 11, 2010, DOI 10.1074/jbc.M110.108167

Jason R. Burke[‡], Alison J. Deshong[‡], Jeffrey G. Pelton[§], and Seth M. Rubin[‡1]

From the [‡]Department of Chemistry and Biochemistry, University of California, Santa Cruz, California 95064 and the [§]California Institute for Quantitative Biosciences, University of California, Berkeley, California 94706

Inactivation of the retinoblastoma protein (Rb) through phosphorylation is an important step in promoting cell cycle progression, and hyperphosphorylated Rb is commonly found in tumors. Rb phosphorylation prevents its association with the E2F transcription factor; however, the molecular basis for complex inhibition has not been established. We identify here the key phosphorylation events and conformational changes that occur in Rb to inhibit the specific association between the E2F transactivation domain ($E2F^{TD}$) and the Rb pocket domain. Calorimetry assays demonstrate that phosphorylation of Rb reduces the affinity of $E2F^{TD}$ binding ~250-fold and that phosphorylation at Ser^{608}/Ser^{612} and Thr^{356}/Thr^{373} is necessary and sufficient for this effect. An NMR assay identifies phosphorylation-driven conformational changes in Rb that directly inhibit $E2F^{TD}$ binding. We find that phosphorylation at Ser^{608}/Ser^{612} promotes an intramolecular association between a conserved sequence in the flexible pocket linker and the pocket domain of Rb that occludes the $E2F^{TD}$ binding site. We also find that phosphorylation of Thr^{356}/Thr^{373} inhibits $E2F^{TD}$ binding in a manner that requires the Rb N-terminal domain. Taken together, our results suggest two distinct mechanisms for how phosphorylation of Rb modulates association between $E2F^{TD}$ and the Rb pocket and describe for the first time a function for the structured N-terminal domain in Rb inactivation.

The retinoblastoma tumor suppressor protein (Rb)[2] is a key negative regulator of cell proliferation, and Rb pathway deregulation is ubiquitous in cancer (1, 2). Rb is inactivated by cyclin-dependent kinases (Cdk) in response to positive growth signals, which results in cell cycle progression (3–6). Rb function as a growth inhibitor in part depends on its ability to repress the transcription activity of E2F (7–10). E2F expression or Rb inactivation induces S phase entry, whereas Rb expression arrests cells in G_1; these observations directly implicate the Rb-E2F pathway as an essential control mechanism of the G_1-S transition and a critical link between growth factor signaling and cell cycle progression (1, 2). In quiescent cells and early G_1, Rb is hypophosphorylated and bound to E2F in a manner that inhibits its transactivation. Phosphorylation of Rb by both Cdk4/6-cyclin D and Cdk2-cyclin E occurs in late G_1 and results in the dissociation of Rb-E2F complexes and E2F activation (4, 5, 11–15). The importance of phosphorylation in Rb inactivation and cellular proliferation is emphasized by the fact that tumor cells often have alterations to upstream regulators that result in Rb hyperphosphorylation (1, 2). However, the molecular basis for how phosphorylation inhibits E2F binding has not been established.

The Rb protein consists of a structured N-terminal domain (RbN) that associates with a structured central domain called the "pocket" (Fig. 1*A*) (16). The C-terminal domain (RbC) is intrinsically disordered (17). Two additional unstructured sequences exist; one is between RbN and the pocket, which we term the interdomain linker (RbIDL), and the other is a linker within the pocket domain (RbPL) that connects the two structured pocket subdomains (18). The Rb-E2F complex is stabilized by two distinct interactions, both of which have been shown to be necessary for growth suppression and inhibition of E2F transcription activity (19, 20). The Rb pocket domain binds the E2F transactivation domain ($E2F^{TD}$) (21, 22), whereas RbC associates with the so-called marked box domains of E2F and its heterodimerization partner DP (Fig. 1*B*) (17).

Human Rb contains 16 Cdk consensus phosphorylation sites, although only a subset of these sites have been found phosphorylated in cells (14). The serine/threonine phosphoacceptor sites are distributed throughout the protein and, with a few exceptions, are in regions of the protein that lack intrinsic structure (Fig. 1*A*). Cell-based assays to uncover the particular phosphorylation events that result in Rb-E2F dissociation and reversal of Rb growth suppression have shown that phosphorylation at many different sites is capable of inactivating Rb (11–13, 23, 24). Insights into the distinct molecular effects of these phosphorylations is therefore critical to understanding the significance of multiple, seemingly redundant pathways toward Rb-E2F dissociation. One possibility is that different phosphorylation events control the two separate Rb-E2F interactions. Indeed, we previously found that phosphorylation of sites in RbC induces an intramolecular interaction between RbC and the pocket domain that specifically blocks the RbC-

* This work was supported, in whole or in part, by National Institutes of Health Grants CA132685 (to S. M. R.) and GM68933 (to support the Central California 900-MHz facility), and SS10-RR20939 (to support the University of California Santa Cruz mass spectrometry facility).

[S] The on-line version of this article (available at http://www.jbc.org) contains supplemental Figs. 1–3.

[1] A Pew Scholar in the Biomedical Sciences, supported by The Pew Charitable Trusts. To whom correspondence should be addressed. Tel.: 831-459-1921; E-mail: srubin@ucsc.edu.

[2] The abbreviations used are: Rb, retinoblastoma protein; phosRb, phosphorylated Rb; dephosRb, dephosphorylated Rb; Cdk, cyclin-dependent kinase(s); MS/MS, tandem mass spectrometry; ITC, isothermal titration calorimetry.

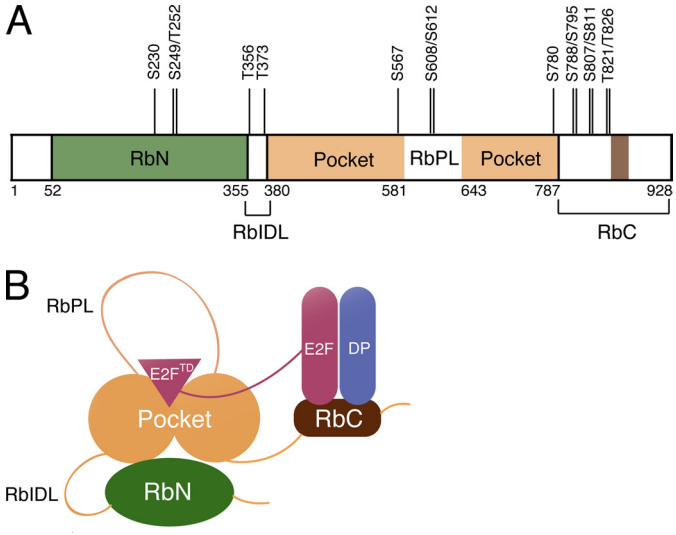

FIGURE 1. **Domain structure of Rb and interactions with E2F-DP.** *A*, Rb consists of a structured N-terminal domain (RbN) and central pocket domain. Its C-terminal domain (RbC) is disordered except for a short sequence that adopts a structure upon E2F binding. Two other unstructured sequences, the interdomain linker (RbIDL) and pocket linker (RbPL), are indicated. Structured regions are *colored*, and the conserved consensus Cdk phosphorylation sites are *marked*. *B*, Rb makes two distinct contacts with E2F. The pocket domain binds the E2F transactivation domain ($E2F^{TD}$), and RbC binds the E2F-DP marked box domains.

marked box association (17). It has also been shown that phosphorylation of sites in the pocket domain is capable of reducing $E2F^{TD}$ binding (22).

Here, we identify unambiguously the key phosphorylation events and characterize the domain rearrangements in Rb that result in inhibition of the $E2F^{TD}$-pocket domain association. Phosphorylation of Thr^{356}/Thr^{373} in RbIDL and Ser^{608}/Ser^{612} in RbPL are each sufficient for partial inhibition of $E2F^{TD}$ binding, but both are necessary for complete inhibition. We show that phosphorylation stimulates an intramolecular interaction between RbPL and the pocket domain that overlaps with the $E2F^{TD}$ binding site. Our data confirm a role for RbPL, RbIDL, and the structured RbN in Rb inactivation and provide the first molecular insights into how phosphorylation disrupts a key cell cycle and growth regulatory complex.

EXPERIMENTAL PROCEDURES

Protein Expression and Purification—Human Rb constructs containing a single domain (*e.g.* RbN or pocket domain) could be expressed with high yields in *Escherichia coli*. Constructs containing multiple domains required expression in Sf9 cells to obtain quantities suitable for biophysical assays. Thus, Rb^{55-928}, Rb^{55-787} (wild type and mutants), and $Rb^{380-928}$ were all expressed in Sf9 cells as His_6 fusion proteins. Cells were infected at a density of $\sim 2 \times 10^6$/ml with baculovirus containing the desired gene and incubated for 2–3 days. Proteins were purified by Ni^{2+}-nitrilotriacetic acid affinity purification and heparin sulfate chromatography. $Rb^{352-787}$, $Rb^{380-787}$ (wild type and mutants), and $RbP^{\Delta PL}$ ($Rb^{380-787}$, with 578–642 deleted) were expressed in *E. coli* as glutathione *S*-transferase fusion proteins. Cells were induced overnight at room temperature. The proteins were purified with glutathione affinity chromatography, the glutathione *S*-transferase tag was cut off, and the Rb domain was isolated by heparin sulfate chromatography. $RbPL^{592-624}$, $Rb^{338-379}$, Rb^{55-379}, and $E2F^{TD}$ (E2F1, residues 372–437) were expressed as His_6 fusion proteins in *E. coli*. Cells were induced for 2–4 h at 37 °C, and proteins were purified by Ni^{2+}-nitrilotriacetic acid affinity and anion exchange chromatography. Isotopically labeled $RbP^{\Delta PL}$ and $RbPL^{592-624}$ were prepared for NMR as described, except that upon induction, *E. coli* were switched to M9 minimal medium including [^{15}N]ammonium chloride, [^{13}C]glucose, and D_2O as necessary. PP1 catalytic domain (α isoform) was expressed in *E. coli* and purified with anion exchange and heparin sulfate chromatography. Recombinant Cdk6-CycK (herpesvirus cyclin) and Cdk2-CycA were expressed and purified as described previously (25, 26).

Enzymatic Modifications—Rb protein constructs were concentrated to ~1–5 mg/ml following purification and then phosphorylated in a reaction containing 10 mM $MgCl_2$, 10 mM ATP, 250 mM NaCl, 25 mM Tris (pH 8.0), and 2% Cdk6-CycK or 10% Cdk2-CycA (percentage of mass of the total substrate in the reaction). Reactions were incubated at room temperature for 1 h. Use of either kinase resulted in similar phosphate incorporation in the reaction described in supplemental Fig. 1. Kinase-treated Rb^{55-928} was digested with either trypsin or chymotrypsin and analyzed for phosphate incorporation using a Thermo Finnigan liquid chromatography/MS/MS (LTQ) linear ion trap. All MS/MS spectra were processed using Bioworks 3.3. Peptide identifications with better than 0.01 peptide probability were accepted and manually inspected.

Phosphatase reactions were carried out with 10% PP1 (percentage of mass of substrate) in the presence of 1 mM $MnCl_2$, 250 mM NaCl, 25 mM Tris (pH 8.0) at room temperature for 1 h. We have found by mass spectrometry and radioisotope labeling assays that these conditions lead to nearly quantitative dephosphorylation (data not shown). Initially, proteins were purified following the enzymatic treatment and prior to isothermal titration calorimetry (ITC) or NMR with size exclusion chromatography; subsequently it was found this step was not necessary because results were unaffected by the purification step.

ITC—ITC experiments were conducted with a MicroCal VP-ITC calorimeter. Typically, ~0.5–1 mM $E2F^{TD}$ and 25–50 μM Rb were used in each experiment. Proteins were dialyzed overnight prior to the assay in a buffer containing 100 mM NaCl, 1 mM dithiothreitol, and 25 mM Tris (pH 8.0). Data were analyzed with the Origin calorimetry software package assuming a one-site binding model. *n* values, reflecting the stoichiometry of the Rb-$E2F^{TD}$ complex, were between 0.8 and 1.2. Experiments were repeated for each Rb construct 2–4 times, and the reported error is the S.D. of each set of measurements.

NMR Spectroscopy—Purified Rb protein constructs were dialyzed into an NMR buffer containing 50 mM sodium phosphate, 5 mM dithiothreitol, and 10% D_2O (pH 6.1). For binding experiments involving labeled $RbPL^{592-624}$, HSQC spectra were recorded at 25 °C on a Varian INOVA 600-MHz spectrometer equipped with an HCN 5-mm cryoprobe (27). Experiments observing labeled $RbP^{\Delta PL}$ and experiments to assign $RbPL^{592-624}$ were conducted with an Avance II 900-MHz spectrometer (Bruker-Biospin, Boston, MA) at the Central California 900-MHz NMR facility (Berkeley, CA). The amide resonances were

assigned via ^{1}H-^{15}N to side chain correlations observed in two-dimensional ^{1}H-^{15}N HSQC-TOCSY (100-ms mixing time) and two-dimensional ^{1}H-^{15}N HSQC-NOESY (350-ms mixing time) experiments and via ^{13}Ca (i, $i-1$) and ^{13}Cb (i, $i-1$) linkages observed in a three-dimensional HNCACB experiment (28–30). NMR spectra were processed with NMRPipe and analyzed with NMRViewJ (31, 32).

RESULTS

RbN Is Required for Phosphorylation-induced Inhibition of E2F^{TD} Binding—To determine the precise sequences and phosphorylation sites within Rb required for inhibition of E2F^{TD} binding, we applied an ITC assay to quantitatively measure affinities with purified proteins. We first expressed in Sf9 insect cells an Rb construct containing amino acids 55–928 (Rb$^{55-928}$). Rb$^{55-928}$ contains all three domains of Rb and all 15 conserved Cdk consensus sites. Rb$^{55-928}$ is phosphorylated by endogenous Sf9 kinases (33), so Rb$^{55-928}$ was dephosphorylated with the Rb phosphatase PP1. As seen in Fig. 2*A*, the affinity of E2F^{TD} for the PP1-treated protein (dephosRb$^{55-928}$) is K_d = 0.04 ± 0.02 μM. This value is comparable with the affinity of E2F^{TD} for unphosphorylated pocket domain purified from bacteria (Rb$^{380-787}$; K_d = 0.045 ± 0.007 μM), which is the Rb domain necessary and sufficient for E2F^{TD} binding (21, 22).

We next phosphorylated Rb$^{55-928}$ with recombinant Cdk-cyclin using reaction conditions that result in quantitative phosphorylation of accessible Cdk consensus sites (supplemental Fig. 1). Phosphorylation was detected at 13 of 15 Cdk consensus sites using phosphopeptide mapping with liquid chromatography/MS/MS (Table 1). Notably, we did not detect phosphorylation at Ser^{230} or Ser^{567} despite the large quantity of purified kinase used in the reaction. Both sites are buried in structured domains and have not been observed to be phosphorylated *in vivo* (14, 21, 22, 34). Calorimetric assays show that E2F^{TD} binds to phosRb$^{55-928}$ with K_d = 11 ± 3 μM (Fig. 2*A*), which is ~250-fold weaker than its association with dephosRb$^{55-928}$ or unphosphorylated Rb$^{380-787}$. This result supports a large body of experiments demonstrating loss of E2F binding to Rb upon Cdk phosphorylation (4, 5, 11–15).

To identify which Rb domains are required for inhibiting E2F^{TD} association, we carried out a series of ITC experiments using Rb truncation mutants that were phosphorylated in our recombinant Cdk reaction. The results of these assays are summarized in Fig. 2*B*, and sample ITC data are shown in supplemental Fig. 2. E2F^{TD} binds an RbC truncation mutant (phosRb$^{55-787}$) with K_d = 13 ± 3 μM, indicating that deletion of RbC has no effect on the phosphorylation-induced change in E2F^{TD} affinity. Therefore, association of phosRbC with the pocket domain is not necessary for inhibition of E2F^{TD} binding, although it remains possible that it has a redundant effect. Part of RbC binds the E2F-DP marked box domains, and previous data demonstrate that RbC phosphorylation specifically inhibits that association (17).

Next, three different N-terminal domain truncation mutants (phosRb$^{380-928}$, phosRb$^{352-787}$, and phosRb$^{380-787}$) were used in binding assays. E2F^{TD} binds significantly tighter to each of these phosphorylated constructs than to phosRb constructs containing the N-terminal domain (Fig. 2*B*). These differences in affinity demonstrate that RbN is required for the full inhibition of E2F^{TD} binding that occurs upon Rb phosphorylation.

Phosphorylation of Thr^{356}/Thr^{373} and Ser^{608}/Ser^{612} Weakens E2F^{TD} Binding to Rb$^{55-787}$—To define further which phosphorylation events are necessary for inhibition of E2F^{TD}-pocket binding, we purified Rb$^{55-787}$ constructs containing alanine mutations such that only specific sites were phosphorylated by kinase. E2F^{TD} binds to wild-type dephosRb$^{55-787}$ with K_d = 0.3 ± 0.2 μM and phosRb$^{55-787}$ with K_d = 13 ± 3 μM (Table 2). Our mass spectrometry data indicate that within residues 55–787, Rb is phosphorylated at Ser^{780} and three pairs of other Cdk consensus sites: Ser^{249}/Thr^{252} in RbN, Thr^{356}/Thr^{373} in RbIDL, and Ser^{608}/Ser^{612} in RbPL (Table 1). We purified and phosphorylated three mutant Rb$^{55-787}$ constructs, each with Ser^{780} and one of the three pairs of phosphoacceptor sites left intact (Table 2). The affinity of E2F^{TD} for the phosRb$^{55-787}$ protein with the Thr^{356}/Thr^{373} and Ser^{608}/Ser^{612} sites mutated (K_d = 0.33 ± 0.02 μM) is equivalent to its affinity for wild-type dephosRb$^{55-787}$. This measurement indicates that Cdk phosphorylation of Ser^{249}, Thr^{252}, and Ser^{780} has no effect on E2F^{TD} binding. The affinities of E2F^{TD} for phosRb$^{55-787}$ with only either Ser^{608}/Ser^{612}/Ser^{780} or Thr^{356}/Thr^{373}/Ser^{780} intact were similar (K_d = 2.7 ± 0.6 μM and K_d = 2.9 ± 0.1 μM, respectively), and both are weaker than wild-type dephosRb$^{55-787}$ but stronger than wild-type phosRb$^{55-787}$. Together these data demonstrate that phosphorylation of Thr^{356}/Thr^{373} and Ser^{608}/Ser^{612} can both partially inhibit E2F^{TD} binding, but neither pair of phosphoacceptor sites is sufficient alone to reproduce the full inhibition observed upon phosphorylation of wild-type protein. To confirm that phosphorylation of both pairs of sites is together sufficient for inhibition, we generated phosRb$^{55-787\Delta 249/252}$ (only Ser^{249}/Thr^{252} mutated) and found that the affinity of E2F^{TD} for this construct (K_d = 25 ± 1 μM) is similar to wild-type phosRb$^{55-787}$ (K_d = 13 ± 3 μM).

It is noteworthy that the E2F^{TD} affinity for phosRb$^{55-787\Delta 249/252}$ is ~25-fold weaker than its affinity for phosRb$^{352-787}$. Both constructs contain the necessary four phosphorylation sites (Thr^{356}, Thr^{373}, Ser^{608}, and Ser^{612}); however, full inhibition of E2F^{TD} binding was only observed for phosRb$^{55-787\Delta 249/252}$, which contains RbN in addition to the required phosphorylation sites. This result suggests further the requirement of RbN for phosphorylation-induced inhibition of E2F, despite the fact that there is no requirement for phosphorylation of the RbN sites. We conclude that the structured RbN must be critical for the mechanism of inhibition.

It is also significant that phosphorylation of Ser^{608}/Ser^{612} causes similar inhibition in the absence of RbN (~15-fold; compare in Fig. 2 K_d values for Rb$^{380-787}$ and phosRb$^{380-787}$) and in the presence of RbN (~9 fold; compare in Table 2 K_d values for dephosRb$^{55-787}$ and phosRb$^{55-787\Delta 249/252/356/373}$). Therefore, the effect of Ser^{608}/Ser^{612} phosphorylation does not require RbN. In sum, our data demonstrate two distinct and independent mechanisms for E2F^{TD} inhibition, each relying on phosphorylation of a specific pair of sites (Thr^{356}/Thr^{373} or Ser^{608}/Ser^{612}).

Phosphorylation Mediates Binding of RbPL to the Rb Pocket Domain—Having identified the required phosphorylation events for E2F^{TD} inhibition, we next explored the conforma-

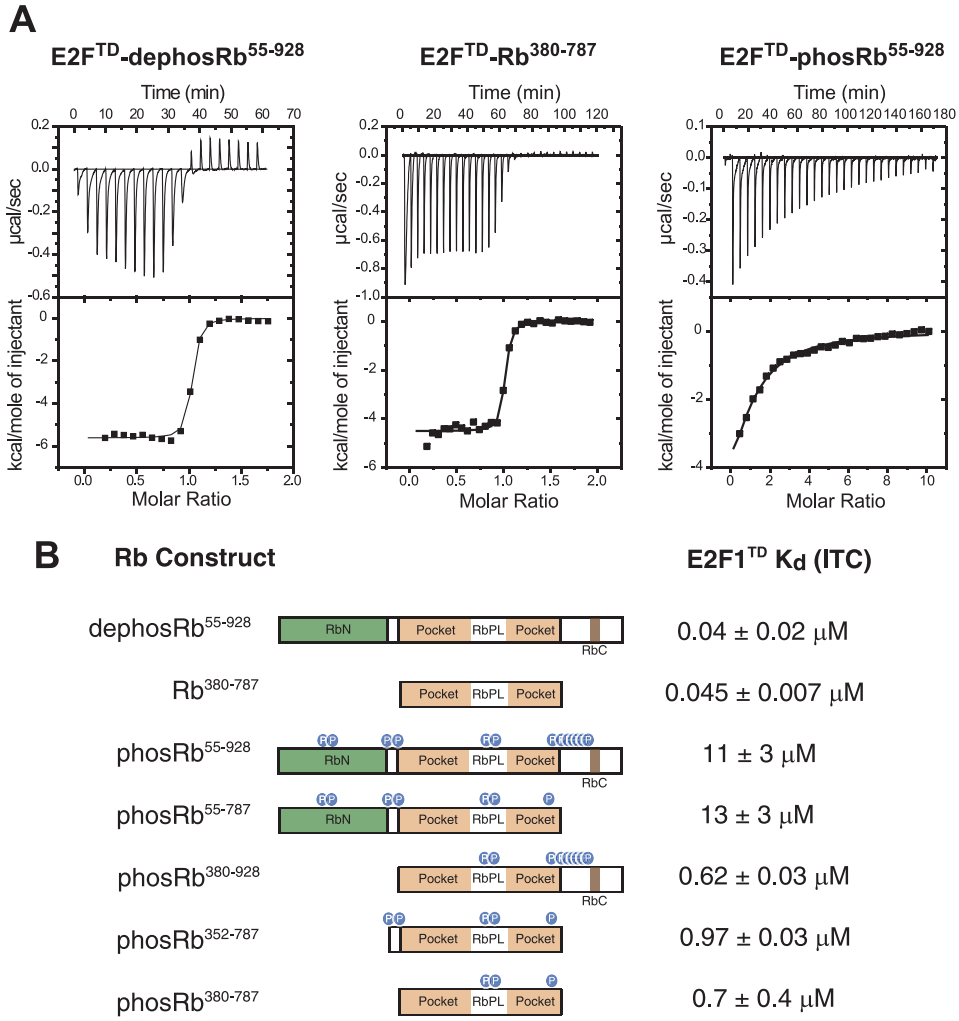

FIGURE 2. **Rb domain requirements for inhibition of E2F^{TD}.** *A*, ITC titration curves show that E2F^{TD} binds to enzymatically dephosphorylated Rb$^{55-928}$ (Rb$^{55-928}$; $K_d = 0.04 \pm 0.02$ μM) with a similar affinity as to the unphosphorylated Rb pocket domain (dephosRb$^{380-787}$; $K_d = 0.045 \pm 0.007$ μM). Phosphorylation of Rb$^{55-928}$ results in a weaker affinity (phosRb$^{55-928}$; $K_d = 11 \pm 3$ μM). *B*, E2F^{TD} dissociation constants were measured by ITC for binding to truncation mutants of Rb. The data demonstrate that RbN is required for phosphorylation-induced inhibition of E2F^{TD}.

tional changes in Rb that cause inhibition. The calorimetry data indicate that the partial inhibition induced by phosphorylation of Ser^{608}/Ser^{612} does not require RbN. Ser^{608} and Ser^{612} are located in RbPL, which comprises a disordered stretch of amino acids linking the two pocket subdomains (Fig. 1*A*). We hypothesized that phosphorylation induces an intramolecular association between the phosphorylated sequence in the linker and the pocket in a manner analogous to that previously observed for phosRbC (17).

To test this model, we attempted to detect a weak interaction between isolated, phosphorylated RbPL and the pocket domain in *trans*. ITC experiments titrating phosRbPL into the Rb pocket domain did not yield any significant heat signal (data not shown). Alternatively, we applied an NMR assay that is more sensitive in detecting the anticipated weak intermolecular association. We first generated a uniformly ^{15}N-labeled phosRbPL$^{592-624}$ construct that contains the phosphorylation sites Ser^{608} and Ser^{612} as well as the only sequence of conserved amino acids within RbPL (Fig. 3*A*). The ^{1}H-^{15}N HSQC spectrum of phosRbPL$^{592-624}$ shows little chemical shift dispersion in the ^{1}H dimension; this observation is consistent with a lack of structure in the pocket linker (Fig. 3*B*). We next purified a pocket domain construct (RbP$^{\Delta PL}$), previously used in crystallization experiments (21, 22), in which the entire RbPL is deleted. Superposition of the HSQC spectrum of phosRbPL$^{592-624}$ alone (Fig. 3*B*, *black*) and a spectrum of phosRbPL$^{592-624}$ in the presence of unlabeled RbP$^{\Delta PL}$ (Fig. 3*B*, *red*) shows that chemical shift changes and peak broadening occur in the presence of Rb pocket. This observation is consistent with binding on the fast to intermediate exchange time scale and the increased correlation time of forming a complex. When the HSQC experiment is repeated using unphosphorylated RbPL$^{592-624}$, no spectral changes are observed in the presence of RbP$^{\Delta PL}$, indicating that the association is phosphorylation-dependent (Fig. 3*C*).

phosRbPL Associates with the Pocket Domain at the E2F^{TD} Binding Site—We next tested whether phosRbPL$^{592-624}$ and E2F^{TD} directly compete for binding to the Rb pocket. Excess E2F^{TD} was added to the sample containing both ^{15}N-labeled phosRbPL$^{592-624}$ and unlabeled RbP$^{\Delta PL}$ pocket. The resulting spectrum (Fig. 3*D*, *red*) shows reduced peak broadening compared with the spectrum taken without E2F^{TD} (Fig. 3*B*, *red*).

This observation is consistent with excess $E2F^{TD}$ displacing $phosRbPL^{592-624}$ from the pocket domain such that the spectrum in the presence of $E2F^{TD}$ resembles that of free $phosRbPL^{592-624}$ (Fig. 3*D*, *black*). $phosRbPL^{592-624}$ and $E2F^{TD}$ thus do not bind simultaneously to the pocket domain. The NMR and calorimetry data together demonstrate that RbPL phosphorylation induces a phosRbPL-pocket association that inhibits $E2F^{TD}$ binding.

Upon assigning the HSQC peaks to specific amino acids in $RbPL^{592-624}$, comparison of peak broadening reveals that the effect is most dramatic for Thr^{601}–Val^{610} (Fig. 3*B*). Residues Asp^{604}–Tyr^{606} are well conserved in orthologs (Fig. 3*A*) and have some sequence similarity to residues Asp^{425}–Phe^{427} of the C terminus of $E2F1^{TD}$. The DLF sequence in $E2F1^{TD}$ makes critical binding contacts to Phe^{482} and Arg^{467} in the pocket domain of Rb (Fig. 4*A*) (21). We supposed that phosRbPL also binds at this site in the pocket. To test this idea, we compared peak broadening in HSQC spectra of ^{15}N-labeled phosRbPL in the presence of unlabeled $RbP^{\Delta PL}$, $RbP^{\Delta PL/F482A}$, and $RbP^{\Delta PL/R467A}$ (Fig. 4). The $RbP^{\Delta PL}$ mutants do not induce the significant peak broadening that is observed with the wild type Rb pocket, suggesting that the affinity of the mutant constructs for phosRbPL is weaker. These data demonstrate that Phe^{482} and Arg^{467} are important for mediating binding between phosRbPL and the pocket and accordingly that the phosRbPL and $E2F^{TD}$ binding sites in the pocket domain overlap.

TABLE 1

Identification of Rb^{55-928} phosphorylation sites following the recombinant kinase reaction

Residue	Phosphorylated[a]	Peptide sequence
230[b]	N	F ↓ IKLSPPML ↓ L
249, 252	Y, Y	K ↓ TAVIPINGS*PRT*PR ↓ R[c]
356	Y	R ↓ LFLDHDKTLQTDSIDSFETQRT*PR ↓ K
373	Y	R ↓ KSNLDEEVNVIPPHT*PVR ↓ T
567	N	R ↓ IMESLAWLSDSPLFDLIK ↓ Q
608, 612[b]	Y, Y	L ↓ NLPLQNNHTAADMYLS*PVRS*PK ↓ K
780	Y	K ↓ TNILQYASTRPPTLS*PIPHIPR ↓ S
788[b]	Y	L ↓ SPIPHIPRS*PY ↓ K
795[b]	Y	Y ↓ KFPSS*PLR ↓ I
807, 811	Y, Y	R ↓ IPGGNIYIS*PLKS*PYK ↓ I
821	Y	K ↓ ISEGLPT*PTK ↓ M
826	Y	K ↓ ISEGLPTPTKMT*PR ↓ S

[a] N, unphosphorylated; Y, phosphorylated; Y, Y, phosphorylated at two sites.
[b] Recovered with chymotrypsin plus trypsin.
[c] Asterisks represent phosphorylation sites identified by MS/MS.

TABLE 2

ITC measurements of $E2F^{TD}$ binding to mutants of $phosRb^{55-787}$

Construct	Mutations	Accessible phosphorylation sites	$E2F^{TD}$ K_d
			μM
$dephosRb^{55-787}$	None	NA[a]	0.3 ± 0.2
$phosRb^{55-787}$	None	Ser^{249}, Thr^{252}, Thr^{356}, Thr^{373}, Ser^{608}, Ser^{612}, Ser^{780}	13 ± 3
$phosRb^{55-787\Delta356/373/608/612}$	T356A, T373A, S608A, S612A	Ser^{249}, Thr^{252}, Ser^{780}	0.33 ± 0.02
$phosRb^{55-787\Delta249/252/356/373}$	S249A, T252A, T356A, T373A	Ser^{608}, Ser^{612}, Ser^{780}	2.7 ± 0.6
$phosRb^{55-787\Delta249/252/608/612}$	S249A, T252A, S608A, S612A	Thr^{356}, Thr^{373}, Ser^{780}	2.9 ± 0.1
$phosRb^{55-787\Delta249/252}$	S249A, T252A	Thr^{356}, Thr^{373}, Ser^{608}, Ser^{612}, Ser^{780}	25 ± 1

[a] Not applicable.

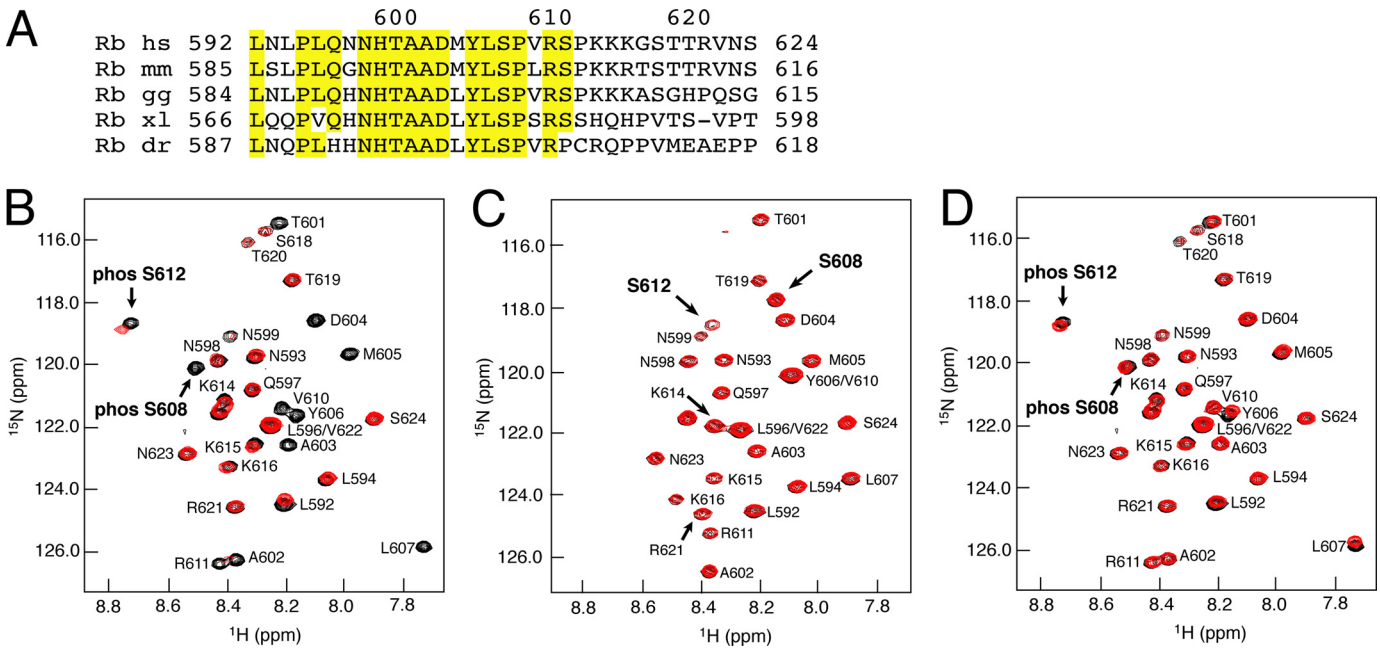

FIGURE 3. **phosRbPL associates with the Rb pocket domain and competes with $E2F^{TD}$ binding.** *A*, alignment of RbPL sequences from human (*hs*), mouse (*mm*), chicken (*gg*), frog (*xl*), and zebrafish (*dr*) shows that residues 595–611 (human) are highly conserved (*yellow*). *B*, HSQC spectra of 100 μM ^{15}N-labeled $phosRbPL^{592-624}$ alone (*black*) and in the presence of 500 μM unlabeled $RbP^{\Delta PL}$ (*red*). Broadening of amide resonances occurs selectively for residues 601–610, indicating a binding interaction between the phosphorylated pocket linker and pocket domain in *trans*. *C*, spectra of 100 μM ^{15}N-labeled unphosphorylated RbPL alone (*black*) and in the presence of 400 μM unlabeled $RbP^{\Delta PL}$ (*red*). No resonance peak broadening is observed for unphosphorylated RbPL in the presence of the Rb pocket, demonstrating that binding is mediated by phosphorylation of RbPL. *D*, spectra of 100 μM ^{15}N-labeled phosRbPL alone (*black*) and with 500 μM unlabeled $RbP^{\Delta PL}$ and 2 mM unlabeled $E2F^{TD}$ (*red*). In the presence of excess $E2F^{TD}$, resonance peaks at chemical shifts corresponding to unbound phosRbPL reappear, indicating that $E2F^{TD}$ competes with phosRbPL for binding to the Rb pocket.

To confirm an important role for residues Asp^{604}–Leu^{607} in the inhibition of E2F^{TD} binding, we tested the affinity of E2F^{TD} for Rb$^{380-787}$ mutants in which these residues were mutated to alanine individually or in combination (Table 3). E2F^{TD} binds phosphorylated wild-type Rb$^{380-787}$ (K_d = 0.7 ± 0.4 μM) with approximately 15-fold less affinity than unphosphorylated protein (K_d = 0.045 ± 0.007 μM). E2F^{TD} binds all of the unphosphorylated mutant proteins in Table 3 with similar affinity as wild type (data not shown). We found that mutation of Met^{605} had little effect on the affinity of E2F^{TD} for phosphorylated Rb pocket, whereas mutation of Asp^{604}, Tyr^{606}, and Leu^{607} each had a modest effect. Mutation of Asp^{604}–Tyr^{606} in combination produced an Rb pocket construct in which phosphorylation does not inhibit E2F^{TD} binding significantly. We conclude that Asp^{604}, Tyr^{606}, and Leu^{607} all probably contribute to the mechanism of E2F^{TD} inhibition due to Rb phosphorylation at Ser^{608}/Ser^{612}.

Finally, we asked whether phosphorylation at Ser^{608} and Ser^{612} are both required for inhibiting binding between E2F^{TD} and the Rb pocket. We constructed serine to alanine mutants for Ser^{608} and Ser^{612} separately and used ITC to quantify changes in E2F^{TD}-phosRb$^{380-787}$ binding (Table 3). The phosphorylated S612A mutant has a similar affinity for E2F^{TD} (K_d = 0.7 ± 0.1 μM) as wild type phosRb$^{380-787}$ (K_d = 0.7 ± 0.4 μM), whereas the phosphorylated S608A mutant does not bind E2F^{TD} as weakly (K_d = 0.15 ± 0.01 μM). These data indicate that Ser^{608} phosphorylation is sufficient for E2F^{TD} inhibition, whereas Ser^{612} phosphorylation has only a modest effect.

The phosRbPL and phosRbN-RbIDL Binding Sites in the Pocket Domain Each Partially Overlap with the E2F^{TD} Binding Site—Our ITC data demonstrate that RbN and phosphorylation at the RbIDL sites are together capable of inhibiting E2F^{TD} binding. We examined whether phosRbN-RbIDL (phosRb$^{55-379}$) associates with the pocket by conducting NMR experiments that monitor signals from the pocket domain. A uniformly labeled ^{2}D-^{15}N sample of RbP^{ΔPL} results in a well resolved ^{1}H-^{15}N TROSY spectrum (supplemental Fig. 3) (35). We compared the effects of the addition of unlabeled

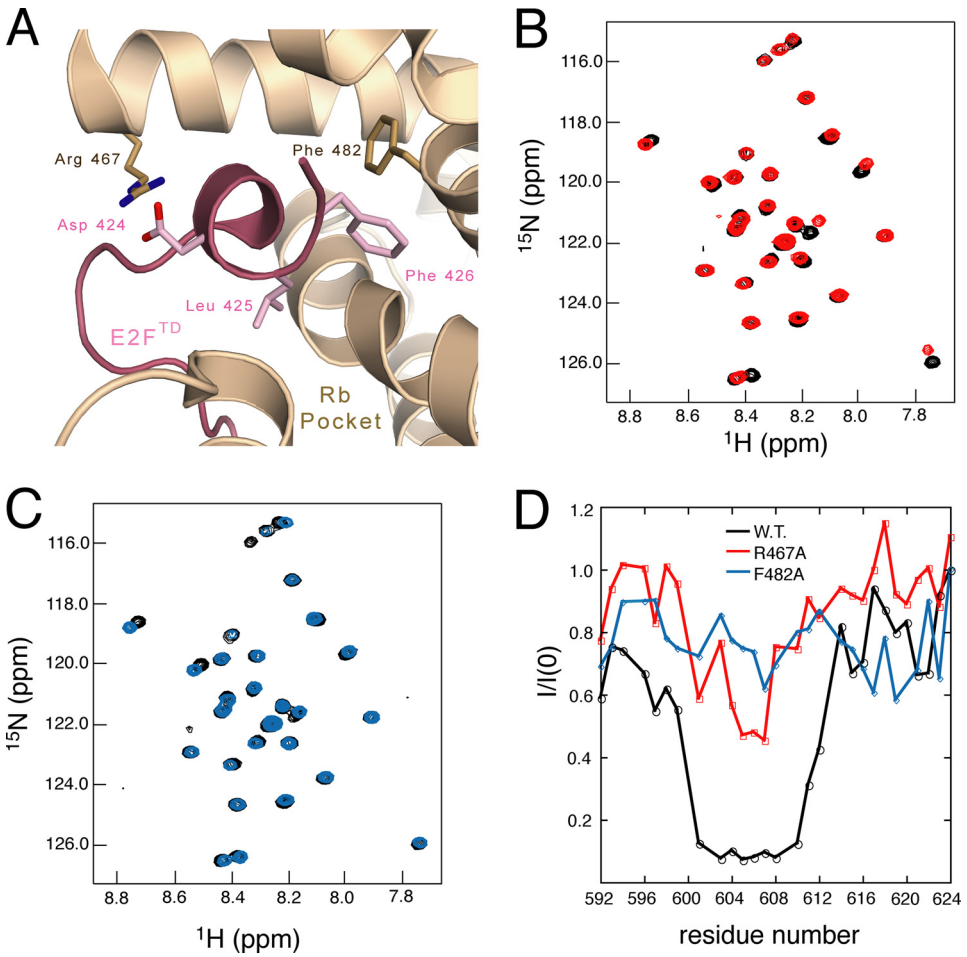

FIGURE 4. **phosRbPL binds the pocket domain at the E2F^{TD} binding site.** *A*, structure of E2F^{TD} bound to the pocket domain. Critical contacts between Asp^{424} and Phe^{426} of E2F and Arg^{467} and Phe^{482} of Rb are shown. This figure was generated using Protein Data Bank entry 1N4M. *B* and *C*, HSQC spectra of 100 μM ^{15}N-labeled phosRbPL$^{592-624}$ alone (*black*) and in the presence of 500 μM unlabeled RbP$^{ΔPL-R467A}$ (*red*) and RbP$^{ΔPL-F482A}$ (*blue*), respectively. *D*, resonance peak intensity ratios of phosRbPL in the presence of wild type RbP^{ΔPL} (*black*) and mutants R467A (*red*) and F482A (*blue*). The ratio I/I_0 is defined as the peak intensity of phosRbPL in the presence of RbP^{ΔPL} (I) divided by the peak intensity of phosRbPL alone (I_0). These data demonstrate that Arg^{467} and Phe^{482} in the pocket domain are critical for binding phosRbPL as well as E2F^{TD}.

TABLE 3
ITC measurements of E2F^{TD} binding to mutants of phosRb$^{380-787}$

Construct	Mutations	Accessible phosphorylation sites	E2F^{TD} K_d
unphosRb$^{380-787}$	None	NA[a]	0.045 ± 0.007 μM
phosRb$^{380-787}$	None	Ser^{608}, Ser^{612}, Ser^{780}	0.7 ± 0.4 μM
phosRb$^{380-787Δ604}$	D604A	Ser^{608}, Ser^{612}, Ser^{780}	0.4 ± 0.2 μM
phosRb$^{380-787Δ605}$	M605A	Ser^{608}, Ser^{612}, Ser^{780}	0.9 ± 0.2 μM
phosRb$^{380-787Δ606}$	Y606A	Ser^{608}, Ser^{612}, Ser^{780}	0.22 ± 0.09 μM
phosRb$^{380-787Δ604/605/606}$	D604A, M605A, Y606A	Ser^{608}, Ser^{612}, Ser^{780}	0.11 ± 0.05 μM
phosRb$^{380-787Δ607}$	L607A	Ser^{608}, Ser^{612}, Ser^{780}	0.3 ± 0.2 μM
phosRb$^{380-787Δ608}$	S608A	Ser^{612}, Ser^{780}	0.15 ± 0.01 μM
phosRb$^{380-787Δ612}$	S612A	Ser^{608}, Ser^{780}	0.7 ± 0.1 μM
phosRb$^{380-787Δ608/612}$	S608A, S612A	Ser^{780}	0.06 ± 0.04 μM

[a] Not applicable.

phosRbN-RbIDL (Fig. 5*A*), phosRbPL (Fig. 5*B*), or E2F^{TD} (Fig. 5*C*) on the spectrum (full spectra in supplemental Fig. 3). Titration of unlabeled phosRb$^{55–379}$ or phosRbPL results in peak broadening indicative of binding with an intermediate exchange time scale. The subset of peaks that broaden in each experiment is different, suggesting that the manner in which phosRbPL and the pocket domain associate is distinct from how phosRb$^{55–379}$ associates with the pocket. Interestingly, the peaks that broaden upon the addition of both phosRbN-RbIDL and phosRbPL also undergo chemical shift changes upon the addition of E2F^{TD} (Fig. 5*C*). This observation suggests that the phosRbN-RbIDL and phosRbPL binding sites in the pocket domain partially overlap with the E2F^{TD} binding site. Binding of both has an independent and additive effect toward E2F^{TD} inhibition, as observed in the calorimetry experiments.

DISCUSSION

We have applied a calorimetry assay with purified proteins to identify unequivocally which phosphorylation events in Rb are capable of inhibiting E2F^{TD} binding, and our data reveal two distinct mechanisms for this inhibition. In the first mechanism, Ser^{608}/Ser^{612} phosphorylation induces an intramolecular association between RbPL and the pocket domain. This association occludes the E2F^{TD} binding site in the pocket such that both phosRbPL and E2F^{TD} cannot bind simultaneously. These results mark a novel role for RbPL, which has previously been poorly characterized. Interestingly, both the Rb paralogs p107 and p130 contain linkers in their pocket domains that have a phosphorylation site within a similar sequence context. This homology suggests that a similar phosphorylation-induced structural change may be conserved in the pocket protein family.

The second mechanism for E2F^{TD} inhibition requires both RbN and phosphorylation at sites in RbIDL. Previously, it has been reported that RbN and the Rb pocket domain associate in a manner that is phosphorylation-independent (16). Our data here suggest that RbN and phosRbIDL together bind to the pocket domain in a manner that partially overlaps the E2F^{TD} binding site. Further structural studies are required to examine in detail how phosphorylation changes the interactions between RbN-RbIDL and the pocket.

A critical advantage of our analysis with recombinant proteins is complete control of the sites and extent of phosphorylation. Previous investigations aimed at identifying the critical phosphorylation events that regulate Rb-E2F binding had mixed results (11–13, 23, 24). These studies generally relied on transient transfections of mutagenized proteins in cancer cell lines. Thus, specific conclusions may have been influenced by substoichiometric degrees of phosphorylation at the acceptor sites that varied depending on the mutant and kinase. In an *in vitro* reaction with large quantities of recombinant kinase, we have achieved nearly quantitative phosphate incorporation, allowing unambiguous interpretation of the molecular effects of phosphorylation. Nevertheless, our results agree with and further explain several key observations from these previous cellular assays. Importantly, in transfection experiments assaying E2F binding, repression of E2F transcription, and growth suppression, cumulative mutation of multiple phosphoacceptor sites was required to abolish the effect of Cdk phosphorylation (11, 13, 23, 24). With previous results, our data reveal that multiple phosphorylation events (Thr^{356}/Thr^{373}, Ser^{608}/Ser^{612}, Ser^{788}/Ser^{795}, and Thr^{821}/Thr^{826}) are capable of inhibiting one of the two interfaces stabilizing the overall complex (Fig. 1), and thus many different combinations of Cdk phosphorylation must all be sufficient to inactivate Rb by disrupting the complex.

Previous studies, which analyzed the effects of Rb phosphorylation at specific sites in cancer cell models, support our

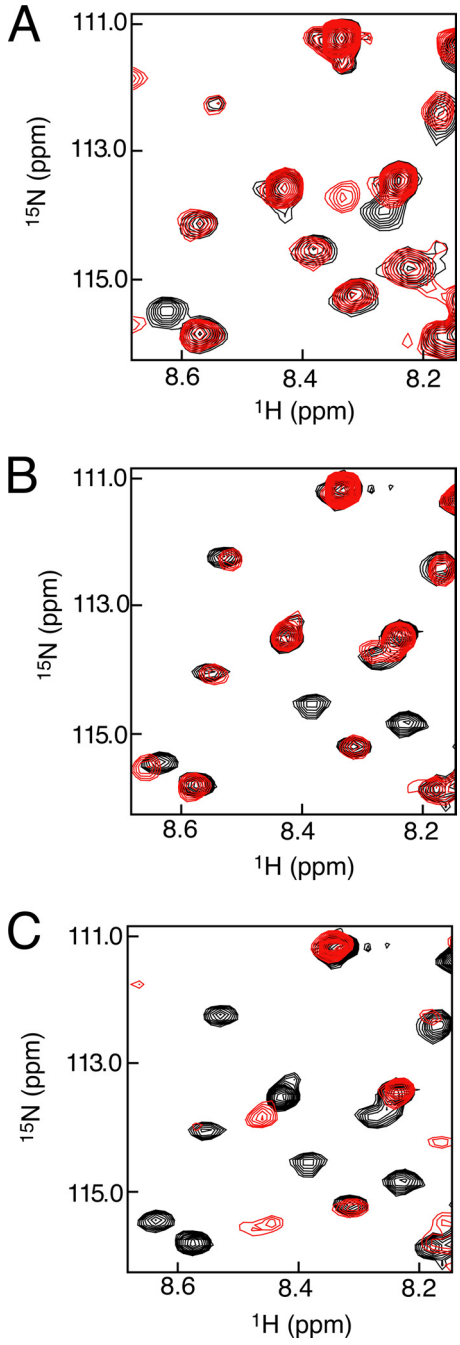

FIGURE 5. **Detail of ^{1}H-^{15}N TROSY spectra of 300 μM ^{2}H-^{15}N-labeled RbP$^{\Delta PL}$ alone (*black*) and in the presence (*red*) of unlabeled phosRbN-RbIDL (400 μM) (*A*), phosRbPL (1.5 mM) (*B*), and E2F^{TD} (2 mM) (*C*).** The observed spectral changes suggest that the binding sites for phosRbN-RbIDL and phosRbPL in the Rb pocket domain each partially overlap with the E2F^{TD} binding site. Full spectra are shown in supplemental Fig. 3.

molecular characterization of Rb-E2F inhibition in several ways. First, phosphorylation reverses Rb repression of E2F-dependent transcription even if all of the RbC sites have been mutated (13, 24). This observation points to a role for phosphorylation outside of RbC in specifically regulating the E2F transactivation domain and is consistent with our calorimetry data. Second, mutation of Ser^{608}/Ser^{612} in addition to all of the RbC sites results in an Rb construct that cannot be regulated by phosphorylation, directly demonstrating the importance of Ser^{608}/Ser^{612} phosphorylation in Rb inactivation (13). Third, Cdk phosphorylation cannot regulate Rb when RbN is deleted and RbC phosphorylation sites are mutated (13). Our data confirm that RbN is required for full phosphorylation-induced $E2F^{TD}$ inhibition. Interestingly, our calorimetry and NMR data suggest that RbN is not required for the partial $E2F^{TD}$ inhibition induced specifically by Ser^{608}/Ser^{612} phosphorylation. One possible explanation for this discrepancy is that the quantitative calorimetry assay used here is more sensitive than the cellular assays in detecting partial inhibition of $E2F^{TD}$ binding.

The implications of multiple possible phosphorylation pathways to E2F dissociation are intriguing. Different phosphorylation sites are probably preferentially phosphorylated by different Cdk-cyclins (34, 36), and thus diverse upstream regulators can affect Rb-E2F stability. On the other hand, although the sites have seemingly redundant roles in combining to inhibit E2F binding, each phosphorylation event is unique in the structural change it induces in Rb. The resulting conformations can differentially influence interactions of Rb with other proteins. For example, the intramolecular association of phosRbC with the pocket domain upon Thr^{821}/Thr^{826} phosphorylation competes with the binding of L*X*C*X*E-containing proteins in addition to inhibiting the RbC-E2F marked box interface (12, 17, 37). Inhibition of the $E2F^{TD}$-pocket association through Ser^{608}/Ser^{612} phosphorylation, however, would still permit L*X*C*X*E protein interactions. Thus, in generating distinct phosphorylated Rb structures, the different E2F inhibition mechanisms resulting from various phosphorylation pathways allow for multiple signaling outputs.

REFERENCES

1. Sherr, C. J. (1996) *Science* **274,** 1672–1677
2. Weinberg, R. A. (1995) *Cell* **81,** 323–330
3. Adams, P. D. (2001) *Biochim. Biophys. Acta* **1471,** M123–133
4. Buchkovich, K., Duffy, L. A., and Harlow, E. (1989) *Cell* **58,** 1097–1105
5. Chen, P. L., Scully, P., Shew, J. Y., Wang, J. Y., and Lee, W. H. (1989) *Cell* **58,** 1193–1198
6. Hinds, P. W., Mittnacht, S., Dulic, V., Arnold, A., Reed, S. I., and Weinberg, R. A. (1992) *Cell* **70,** 993–1006
7. Chellappan, S. P., Hiebert, S., Mudryj, M., Horowitz, J. M., and Nevins, J. R. (1991) *Cell* **65,** 1053–1061
8. Fattaey, A., Helin, K., and Harlow, E. (1993) *Philos Trans. R. Soc. Lond. B Biol. Sci.* **340,** 333–336
9. Flemington, E. K., Speck, S. H., and Kaelin, W. G., Jr. (1993) *Proc. Natl. Acad. Sci. U.S.A.* **90,** 6914–6918
10. Hiebert, S. W., Chellappan, S. P., Horowitz, J. M., and Nevins, J. R. (1992) *Genes Dev.* **6,** 177–185
11. Brown, V. D., Phillips, R. A., and Gallie, B. L. (1999) *Mol. Cell. Biol.* **19,** 3246–3256
12. Harbour, J. W., Luo, R. X., Dei Santi, A., Postigo, A. A., and Dean, D. C. (1999) *Cell* **98,** 859–869
13. Knudsen, E. S., and Wang, J. Y. (1997) *Mol. Cell. Biol.* **17,** 5771–5783
14. Lees, J. A., Buchkovich, K. J., Marshak, D. R., Anderson, C. W., and Harlow, E. (1991) *EMBO J.* **10,** 4279–4290
15. Lundberg, A. S., and Weinberg, R. A. (1998) *Mol. Cell. Biol.* **18,** 753–761
16. Hassler, M., Singh, S., Yue, W. W., Luczynski, M., Lakbir, R., Sanchez-Sanchez, F., Bader, T., Pearl, L. H., and Mittnacht, S. (2007) *Mol. Cell* **28,** 371–385
17. Rubin, S. M., Gall, A. L., Zheng, N., and Pavletich, N. P. (2005) *Cell* **123,** 1093–1106
18. Lee, J. O., Russo, A. A., and Pavletich, N. P. (1998) *Nature* **391,** 859–865
19. Hiebert, S. W. (1993) *Mol. Cell. Biol.* **13,** 3384–3391
20. Qin, X. Q., Chittenden, T., Livingston, D. M., and Kaelin, W. G., Jr. (1992) *Genes Dev.* **6,** 953–964
21. Lee, C., Chang, J. H., Lee, H. S., and Cho, Y. (2002) *Genes Dev.* **16,** 3199–3212
22. Xiao, B., Spencer, J., Clements, A., Ali-Khan, N., Mittnacht, S., Broceño, C., Burghammer, M., Perrakis, A., Marmorstein, R., and Gamblin, S. J. (2003) *Proc. Natl. Acad. Sci. U.S.A.* **100,** 2363–2368
23. Lents, N. H., Gorges, L. L., and Baldassare, J. J. (2006) *Cell Cycle* **5,** 1699–1707
24. Chew, Y. P., Ellis, M., Wilkie, S., and Mittnacht, S. (1998) *Oncogene* **17,** 2177–2186
25. Jeffrey, P. D., Tong, L., and Pavletich, N. P. (2000) *Genes Dev.* **14,** 3115–3125
26. Russo, A. A. (1997) *Methods Enzymol.* **283,** 3–12
27. Mori, S., Abeygunawardana, C., Johnson, M. O., and van Zijl, P. C. (1995) *J. Magn. Reson. B* **108,** 94–98
28. Norwood, T. J., Boyd, J., Heritage, J. E., Soffe, N., and Campbell, I. D. (1990) *J. Magn. Reson.* **87,** 488–501
29. Wittekind, M., and Mueller, L. (1993) *J. Magn. Reson. B* **101,** 201–205
30. Muhandiram, D. R., and Kay, L. E. (1994) *J. Magn. Reson. B* **103,** 203–216
31. Johnson, B. A., and Blevins, R. A. (1994) *J. Biomol. NMR* **4,** 603–614
32. Delaglio, F., Grzesiek, S., Vuister, G. W., Zhu, G., Pfeifer, J., and Bax, A. (1995) *J. Biomol. NMR* **6,** 277–293
33. Lin, B. T., Gruenwald, S., Morla, A. O., Lee, W. H., and Wang, J. Y. (1991) *EMBO J.* **10,** 857–864
34. Zarkowska, T., and Mittnacht, S. (1997) *J. Biol. Chem.* **272,** 12738–12746
35. Singh, M., Krajewski, M., Mikolajka, A., and Holak, T. A. (2005) *J. Biol. Chem.* **280,** 37868–37876
36. Kitagawa, M., Higashi, H., Jung, H. K., Suzuki-Takahashi, I., Ikeda, M., Tamai, K., Kato, J., Segawa, K., Yoshida, E., Nishimura, S., and Taya, Y. (1996) *EMBO J.* **15,** 7060–7069
37. Knudsen, E. S., and Wang, J. Y. (1996) *J. Biol. Chem.* **271,** 8313–8320